Algebraic solutions for $U^{BF}(5)$-$O^{BF}(6)$ quantum phase transition in odd-mass-number nuclei

M. A. Jafarizadeh*
Department of Theoretical Physics and Astrophysics, University of Tabriz, Tabriz 51664, Iran
and Research Institute for Fundamental Sciences, Tabriz 51664, Iran

M. Ghapanvari and N. Fouladi
Department of Nuclear Physics, University of Tabriz, Tabriz 51664, Iran
(Received 26 July 2015; revised manuscript received 21 September 2015; published 16 November 2015)

The spherical to γ-unstable nuclei shape-phase transition in odd-A nuclei is investigated by using the dual algebraic structures and the affine $\widehat{SU(1,1)}$ Lie algebra within the framework of the interacting boson-fermion model. The new algebraic solution for odd-A nuclei is introduced. In this model, single $j = 1/2$ and $3/2$ fermions are coupled with an even-even boson core. Energy spectra, quadrupole electromagnetic transitions, and an expectation value of the d-boson number operator are presented. Experimental evidence for the $U^{BF}(5)$-$O^{BF}(6)$ transition in odd-A Ba and Rh isotopes is presented. The low-states energy spectra and $B(E2)$ values for these nuclei are also calculated and compared with the experimental data.

DOI: 10.1103/PhysRevC.92.054306 PACS number(s): 21.60.Ev, 21.60.Fw, 23.20.Js, 27.60.+j

I. INTRODUCTION

Quantum phase transitions (QPTs) are sudden changes in the structure of a physical system. Nuclear physics has important contributions to make to their study because nuclei display a variety of phases in systems ranging from few to many particles [1]. The signs of QPTs in nuclear physics are changes in the mass and radius of nuclei and quantities such as level crossing and electromagnetic transition rates when the number of protons or neutrons is modified. Phase transition happens in both even-even and odd-A nuclei. Phase transition investigations have been mostly performed on even-even systems [2] within the framework of the interacting boson model (IBM) [2,3], which describes nuclei in terms of correlated pairs of nucleons with $L = 0,2$ treated as bosons (s,d bosons). The IBM Hamiltonian has exact solutions in three dynamical symmetry limits [U(5), SU(3), and O(6)]. These situations correspond to the spherical, axially deformed, and γ-unstable ground-state shapes, respectively. The transition between the U(5) and SU(3) limits is a first-order shape-phase transition while a second-order shape-phase transition occurs between the U(5) and O(6) limits [4–6]. During a transition from one limit to another, the points meet where the potential has flat behavior. These points are called critical points. Recently Iachello introduced the so-called critical point symmetries in the framework of the collective model for even-even nuclei. The critical point from spherical to γ-unstable shapes is called E(5) [3,6], the critical point from spherical to axially deformed shapes is called X(5) [4,6], and the critical point from axially deformed shapes to triaxial shapes is called Y(5) [6,7]. Phase transitions are also investigated in odd-A nuclei within the framework of the interacting boson-fermion model (IBFM) [8,9], which describes nuclei in terms of correlated pairs, with $L = 0,2$ (s,d bosons) and unpaired particles of angular momentum j (j fermions). Studies of QPTs in odd-even nuclei were implicitly initiated years ago by Scholten and Blasi [10]. Several explicit studies were recently made by Alonso *et al.* [11–13] and by Boyukata *et al.* [14], who also suggested a simple form of the IBFM Hamiltonian, particularly well suited to study QPTs in odd-even nuclei because of their supersymmetric properties. Similar to even-even nuclei, there also exists a critical point for odd-even and even-odd nuclei but in this case, critical points show with $E(5/\sum_j 2j+1)$ and $X(5/\sum_j 2j+1)$, where j is the angular momentum of a single nucleon. Iachello [15,16] studied the case of a j (3/2) fermion coupled to a boson core that undergoes a transition from spherical to γ-unstable shapes. At the critical point, an elegant analytic solution, called E(5/4), was obtained starting from the Bohr Hamiltonian [15]. The effect of a fermion on quantum phase transitions of an (s,d) bosonic system is investigated in Ref. [17]. They showed that the presence of a fermion strongly modifies the critical value at which the transition occurs.

In this study, we investigate the transition $U^{BF}(5)$-$O^{BF}(6)$ in odd-A nuclei. The new algebraic solution for odd-A nuclei is introduced. For this transition only the boson core experiences the transition and fermion with $j = 1/2$ and $3/2$ coupled to the boson core. We evaluate exact solutions for eigenstate and energy eigenvalues for the transitional region in the IBFM by using the dual algebraic structure for the two-level pairing model based on the Richardson-Gaudin method and changing the control parameter based on affine $\widehat{SU(1,1)}$ Lie algebra. In order to investigate the phase transition, we calculate observables such as level crossing, expectation values of the d-boson number operator, ground-state energy, and its first derivative. The low-lying states of $^{127-137}_{56}$Ba and $^{101-109}_{45}$Rh isotopes are studied within suggested model. The results of calculations for these nuclei are presented for energy levels and transitions probabilities and two neutron separation energies, and are compared with the corresponding experimental data.

This paper is organized as follows: Sec. II briefly summarizes theoretical aspects of the transitional Hamiltonian and

*jafarizadeh@tabrizu.ac.ir

affine $\widehat{SU(1,1)}$ algebraic technique. Sections III and IV include the results and experimental evidence and Sec. V is devoted to the summary and some conclusions.

II. THEORETICAL FRAMEWORK

The SU(1,1) algebra is explained in detail in Refs. [18–20]. The SU(1,1) algebra is produced by S^ν, $\nu = 0$, and $\pm$, which satisfies the following commutation relations:

$$[S^0, S^\pm] = \pm S^\pm, \quad [S^+, S^-] = -2S^0. \tag{1}$$

The quadratic Casimir operator of SU(1,1) can be written as

$$\hat{C}_2 = S^0(S^0 - 1) - S^+S^-. \tag{2}$$

The basis states of an irreducible representation SU(1,1), $|k\mu\rangle$, are determined by a single number k, where k can be any positive number and $\mu = k, k+1, \ldots$. Therefore [19,20],

$$\hat{C}_2(\mathrm{SU}(1,1))|k\mu\rangle = k(k-1)|k\mu\rangle, \quad S^0|k\mu\rangle = \mu|k\mu\rangle. \tag{3}$$

In IBM, the generators of $\mathrm{SU}^d(1,1)$ are generated by the d-boson pairing algebra:

$$\begin{aligned} S^+(d) &= \frac{1}{2}(d^+.d^+), \quad S^-(d) = \frac{1}{2}(\tilde{d}.\tilde{d}), \\ S^0(d) &= \frac{1}{4}\sum_\nu (d_\nu^+ d_\nu + d_\nu d_\nu^+) = \frac{1}{4}(2\hat{n}_d + 5). \end{aligned} \tag{4}$$

Similarly, s-boson pairing algebra forms another $\mathrm{SU}^s(1,1)$ algebra generated by

$$\begin{aligned} S^+(s) &= \tfrac{1}{2}s^{+^2}, \quad S^-(s) = \tfrac{1}{2}s^2, \\ S^0(s) &= \tfrac{1}{4}(s^+s + ss^+) = \tfrac{1}{4}(2\hat{n}_s + 1). \end{aligned} \tag{5}$$

$\mathrm{SU}^{sd}(1,1)$ is the s- and d-boson pairing algebra generated by

$$\begin{aligned} S^+(sd) &= \frac{1}{2}(d^+.d^+ \pm s^{+^2}), \quad S^-(sd) = \frac{1}{2}(\tilde{d}.\tilde{d} \pm s^2), \\ S^0(sd) &= \frac{1}{4}\sum_\nu (d_\nu^+ d_\nu + d_\nu d_\nu^+) + \frac{1}{4}(s^+s + ss^+). \end{aligned} \tag{6}$$

Because of duality relationships [21,22], it is known that the bases of U(5) ⊃ SO(5) and SO(6) ⊃ SO(5) are simultaneously the basis of $\mathrm{SU}^d(1,1) \supset \mathrm{U}(1)$ and $\mathrm{SU}^{sd}(1,1) \supset \mathrm{U}(1)$, respectively. By use of duality relations [19,21], the Casimir operators of SO(5) and SO(6) can also be expressed in terms of the Casimir operators of $\mathrm{SU}^d(1,1)$ and $\mathrm{SU}^{sd}(1,1)$, respectively:

$$\hat{C}_2(\mathrm{SU}^d(1,1)) = \frac{5}{16} + \frac{1}{4}\hat{C}_2(\mathrm{SO}(5)), \tag{7}$$

$$\hat{C}_2(\mathrm{SU}^{sd}(1,1)) = \frac{3}{4} + \frac{1}{4}\hat{C}_2(\mathrm{SO}(6)). \tag{8}$$

The infinite-dimensional SU(1,1) algebra is generated by use of [19,20]

$$\begin{aligned} S_n^\pm &= c_s^{2n+1}S^\pm(s) + c_d^{2n+1}S^\pm(d), \\ S_n^0 &= c_s^{2n}S^0(s) + c_d^{2n}S^0(d), \end{aligned} \tag{9}$$

where c_s and c_d are real parameters and n can be $0, \pm1, \pm2, \ldots$. These generators satisfy the commutation relations

$$[S_m^0, S_n^\pm] = \pm S_{m+n}^\pm, \quad [S_m^+, S_n^-] = -2S_{m+n+1}^0. \tag{10}$$

Then, $S_m^\mu, \mu = 0, +, -; m = \pm1, \pm2, \ldots$ generate an affine Lie algebra $\widehat{SU(1,1)}$ without central extension.

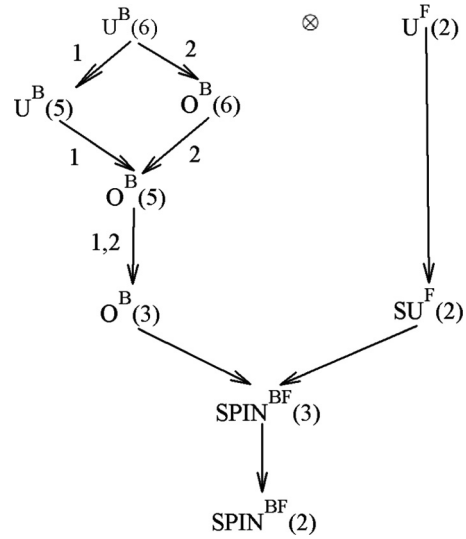

FIG. 1. The lattice of algebras in the case of a system of N bosons (with $L = 0,2$) coupled to a fermion with angular momentum $j = 1/2$.

In odd-A nuclei the Bose-Fermi symmetries are associated with each of the dynamic symmetries of IBM-1 [8]. So, the boson algebraic structure will be always taken to be $\mathrm{U}^B(6)$, while the fermion algebraic structure will depend on the values of the angular momenta, j, taken into consideration [8]. First we considered the case of a system of N bosons (with $L = 0,2$) coupled to a fermion with angular momentum $j = 1/2$. The lattice of algebras in this case is shown in Fig. 1. In Figs. 1 and 2, chain 1 shows the state that bosons have $\mathrm{U}^B(5)$ dynamical symmetry while bosons in chain 2 have $\mathrm{O}^B(6)$ dynamical symmetry. By employing the generators of algebra $\widehat{SU(1,1)}$ and Casimir operators of subalgebras, the following Hamiltonian for the transitional region between $\mathrm{U}^{BF}(5)$ and $\mathrm{O}^{BF}(6)$ limits is prepared:

$$\begin{aligned} \hat{H} = {} & gS_0^+S_0^- + \alpha S_1^0 + \beta\hat{C}_2(\mathrm{SO}^B(5)) \\ & + \delta\hat{C}_2(\mathrm{SO}^B(3)) + \gamma\hat{C}_2(\mathrm{spin}^{BF}(3)). \end{aligned} \tag{11}$$

Following this, we considered the state where the odd nucleon is in a $j = 3/2$ shell. The lattice of algebras in this case is also shown in Fig. 2. The Hamiltonian for the state where the odd nucleon is in a $j = 3/2$ shell for the transitional region between $\mathrm{U}^{BF}(5)$and $\mathrm{O}^{BF}(6)$ limits is

$$\hat{H} = gS_0^+S_0^- + \alpha S_1^0 + \beta\hat{C}_2(\mathrm{spin}^{BF}(5)) + \gamma\hat{C}_2(\mathrm{spin}^{BF}(3)). \tag{12}$$

Equations (11) and (12) are the suggested Hamiltonians for boson-fermion systems with $j = 1/2$ and $3/2$, respectively, and α, β, δ, and γ are real parameters. By considering Eqs. (2), (7), and (8), it can be shown that Hamiltonians (11)

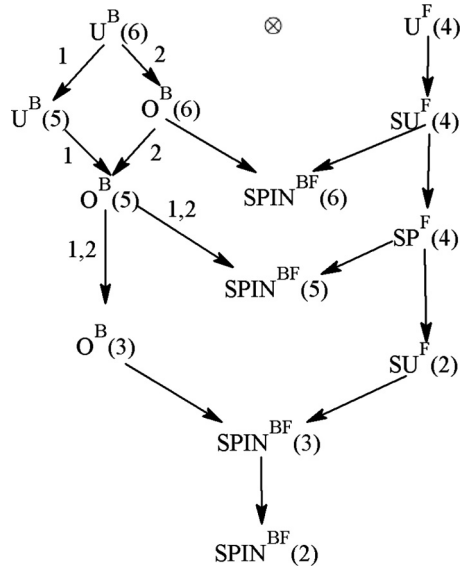

FIG. 2. The lattice of algebras in the case of a system of N bosons (with $L = 0,2$) coupled to a fermion with angular momentum $j = 3/2$.

and (12) are equivalent to the $O^{BF}(6)$ Hamiltonian when $c_s = c_d$ and with the $U^{BF}(5)$ Hamiltonian if $c_s = 0$ and $c_d \neq 0$. Thus, as mentioned, because only the boson core experiences the transition and the fermion is coupled to the boson core, the $c_s \neq c_d \neq 0$ situation just corresponds to the $U^{BF}(5) \leftrightarrow O^{BF}(6)$ transitional region. In our calculation, we take $c_d(=1)$ as a constant value, and c_s changes between 0 and c_d. For evaluating the eigenvalues of Hamiltonians (11) and (12), the eigenstates are considered as [19,20]

$$|k; v_s v n_\Delta LM\rangle = \sum_{n_i \in Z} a_{n_1 n_2 \cdots n_k} x_1^{n_1} x_2^{n_2} x_3^{n_3} \cdots \times x_k^{n_k} S_{n_1}^+ S_{n_2}^+ S_{n_3}^+ \cdots S_{n_k}^+ |lw\rangle. \quad (13)$$

Eigenstates of Hamiltonians (11) and (12) can be obtained by using the Fourier-Laurent expansion of eigenstates and SU(1,1) generators in terms of c unknown number parameters x_i with $i = 1,2,\ldots,k$. It means one can consider the eigenstates as [19,20]

$$|k; v_s v n_\Delta LM\rangle = \mathcal{N} S_{x_1}^+ S_{x_2}^+ S_{x_3}^+ \cdots S_{x_k}^+ |lw\rangle^{BF}, \quad (14)$$

where $\mathcal{N}$ is the normalization factor and

$$S_{x_i}^+ = \frac{c_s}{1 - c_s^2 x_i} S^+(s) + \frac{c_d}{1 - c_d^2 x_i} S^+(d). \quad (15)$$

The c numbers x_i are determined through the following set of equations:

$$\frac{\alpha}{x_i} = \frac{g c_s^2 \left(v_s + \frac{1}{2}\right)}{1 - c_s^2 x_i} + \frac{g c_d^2 \left(v_d + \frac{5}{2}\right)}{1 - c_d^2 x_i} - \sum_{j \neq i} \frac{2g}{x_i - x_j}. \quad (16)$$

With the Clebsch-Gordan (CG) coefficient, we can calculate the lowest weight state, $|\mathrm{lw}\rangle^{BF}$, in terms of boson and fermion parts. For the $j = 1/2$ case we have

$$|\mathrm{lw}\rangle^B_{m\pm\frac{1}{2}} = \left| N, \quad k_d = \frac{1}{2}\left(v_d + \frac{5}{2}\right), \quad \mu_d = \frac{1}{2}\left(n_d + \frac{5}{2}\right), \quad k_s = \frac{1}{2}\left(v_s + \frac{1}{2}\right), \quad \mu_s = \frac{1}{2}\left(n_s + \frac{1}{2}\right), \quad L, m \pm \frac{1}{2} \right\rangle \quad (17)$$

$$|\mathrm{lw}\rangle^{BF} = \pm\sqrt{\frac{L \pm m + \frac{1}{2}}{(2L+1)}} |\mathrm{lw}\rangle^B_{m-\frac{1}{2}} \chi_+ + \sqrt{\frac{L \mp m + \frac{1}{2}}{(2L+1)}} |\mathrm{lw}\rangle^B_{m+\frac{1}{2}} \chi_-. \quad (18)$$

The lowest weight state for the $j = 3/2$ case is calculated as

$$|\mathrm{lw}\rangle^B_{m\pm\frac{3}{2}} = \left| N, k_d = \frac{1}{2}\left(v_d + \frac{5}{2}\right), \quad \mu_d = \frac{1}{2}\left(n_d + \frac{5}{2}\right), \quad k_s = \frac{1}{2}\left(v_s + \frac{1}{2}\right), \quad \mu_s = \frac{1}{2}\left(n_s + \frac{1}{2}\right), \quad L, m \pm \frac{3}{2} \right\rangle, \quad (19)$$

$$|\mathrm{lw}\rangle^{BF} = C^{J,L,\frac{3}{2}}_{m,m-\frac{3}{2},\frac{3}{2}} |\mathrm{lw}\rangle^B_{m-\frac{3}{2}} \left| j = \frac{3}{2}, m_j = \frac{3}{2} \right\rangle + C^{J,L,\frac{3}{2}}_{m,m-\frac{1}{2},\frac{1}{2}} |\mathrm{lw}\rangle^B_{m-\frac{1}{2}} \left| j = \frac{3}{2}, m_j = \frac{1}{2} \right\rangle + C^{J,L,\frac{3}{2}}_{m,m+\frac{1}{2},-\frac{1}{2}} |\mathrm{lw}\rangle^B_{m+\frac{1}{2}} \left| j = \frac{3}{2}, m_j = -\frac{1}{2} \right\rangle + C^{J,L,\frac{3}{2}}_{m,m+\frac{3}{2},-\frac{3}{2}} |\mathrm{lw}\rangle^B_{m+\frac{3}{2}} \left| j = \frac{3}{2}, m_j = -\frac{3}{2} \right\rangle. \quad (20)$$

The $C^{J,L,j}_{m,m_L,m_j}$ symbols represent Clebsch-Gordan coefficients, where

$$S_n^0 |\mathrm{lw}\rangle^{BF} = \Lambda_n^0 |\mathrm{lw}\rangle^{BF}, \quad (21)$$

$$\Lambda_n^0 = c_s^{2n}\left(v_s + \frac{1}{2}\right)\frac{1}{2} + c_d^{2n}\left(v_d + \frac{5}{2}\right)\frac{1}{2}. \quad (22)$$

The eigenvalues of Hamiltonians (11) and (12) can then be expressed:

$$E^{(k)} = h^{(k)} + \alpha\Lambda_1^0 + \beta v_d(v_d + 3) + \delta L(L+1) + \gamma J(J+1), \quad (23)$$

$$E^{(k)} = h^{(k)} + \alpha\Lambda_1^0 + \beta(v_1(v_1+3) + v_2(v_2+1)) + \gamma J(J+1) \quad (24)$$

$$h^{(k)} = \sum_{i=1}^{k} \frac{\alpha}{x_i}. \quad (25)$$

The quantum number (k) is related to the total boson number N by

$$N = 2k + v_s + v_d.$$

In order to obtain the numerical results for energy spectra $(E^{(k)})$ of the considered nuclei, a set of nonlinear Bethe ansatz equations (BAEs) with k unknowns for k-pair excitations must be solved [19,20]; also constants of the Hamiltonian

to experimental data are obtained with the least squares fitting process. To achieve this aim, we have changed variables as follows:

$$C = \frac{c_s}{c_d} \leqslant 1, \quad g = 1, \quad y_i = c_d^2 x_i.$$

So, the new form of Eq. (16) would be

$$\frac{\alpha}{y_i} = \frac{C^2\left(\nu_s + \frac{1}{2}\right)}{1 - C^2 y_i} + \frac{\left(\nu_d + \frac{5}{2}\right)}{1 - y_i} - \sum_{j \neq i} \frac{2}{y_i - y_j}. \tag{26}$$

To calculate the roots of BAEs with specified values of ν_s and ν_d, we solve Eq. (26) with definite values of C and α [18]. Then, we carry out this procedure with different values of C and α to give energy spectra with minimum variation compared to experimental values [23]:

$$\sigma = \left(\frac{1}{N_{\text{tot}}} \sum_{i,\text{tot}} |E_{\text{expt}}(i) - E_{\text{calc}}(i)|^2\right)^{\frac{1}{2}}$$

where N_{tot} is the number of energy levels included in the fitting processes. The method for optimizing the set of parameters in the Hamiltonian (β,γ,δ) includes carrying out a least-squares fit (LSF) of the excitation energies of selected states [18].

III. RESULTS

This section presents the calculated phase transition observables such as level crossing, ground-state energy and the derivative of the energy, expectation values of the d-boson number operator, and energy differences.

A. Energy spectrum and level crossing

To display how the energy levels change as a function of the control parameter C and the total number of bosons, N, the lowest energy levels as a function of C for $N = 10,20$ bosons are shown in Figs. 3 and 4, where in Fig. 3 other fixed parameters are $\alpha = 1000$ keV, $\beta = -57$ keV, $\delta = 41$ keV, and $\gamma = 36$ keV and Fig. 4 is obtained with $\alpha = 1000$ keV, $\beta = 6.5$ keV, and $\gamma = -22$ keV. The figures show how the energy levels as a function of the control parameter C evolve from one dynamical symmetry limit to the other. It can be seen from the figures that numerous level crossings occur, especially in the region around $C \geqslant 0.7$. The crossings are due to the fact that ν_d, the O(5) quantum number with seniority, is preserved along the whole path between O(6) and U(5) [24]. With increasing N, level crossings increase, which is clearly shown in Figs. 3(b) and 4(b).

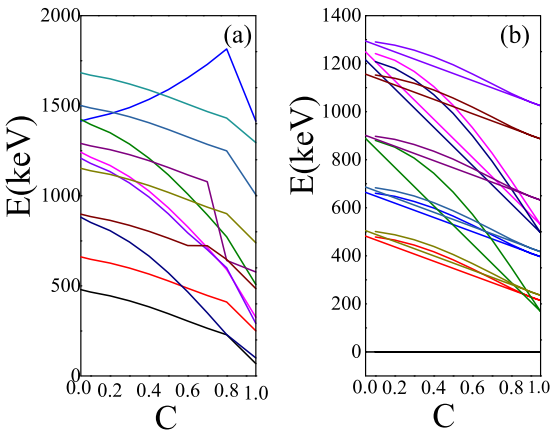

FIG. 3. (Color online) Some low-lying energy levels (in keV) as a function of the control parameter C in the Hamiltonian (11): (a) $N = 10$ bosons and (b) $N = 20$ bosons with $\alpha = 1000$ keV, $\beta = -57$ keV, $\delta = 41$ keV, and $\gamma = 36$ keV.

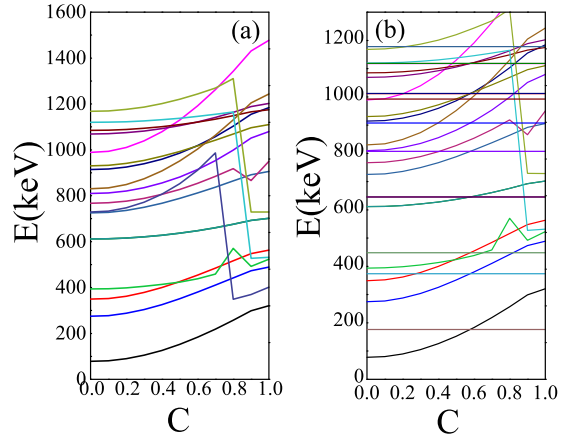

FIG. 4. (Color online) Same as Fig. 3 but with Hamiltonian (12) with $\alpha = 1000$ keV, $\beta = 6.5$ keV, and $\gamma = -22$ keV.

B. Ground-state energy

The ground-state energy is an important observable of phase transitions. So, we calculated the ground-state energy, $E_{\text{g.s.}}$, and its first derivative, $\frac{\partial E_{\text{g.s.}}}{\partial C}$. Figure 5 shows changing of the ground-state energy and its first derivative versus the control parameter C. Both operators, $E_{\text{g.s.}}$ and $\frac{\partial E_{\text{g.s.}}}{\partial C}$, are approximately zero in one phase and different from zero in the other phase. Since a low number of bosons, N, is chosen, it is not possible to distinguish whether the transition is first or second order, as is done in the even-even case [25,26].

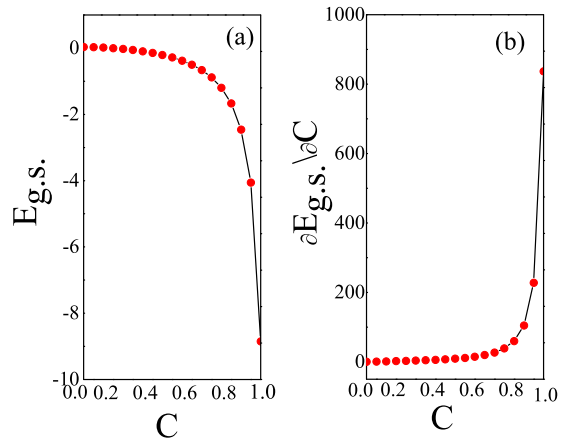

FIG. 5. (Color online) The (a) ground-state energy (in keV) and (b) derivative of the ground-state energy (in keV) presented as a function of the control parameter C for a system with $N = 10$ bosons.

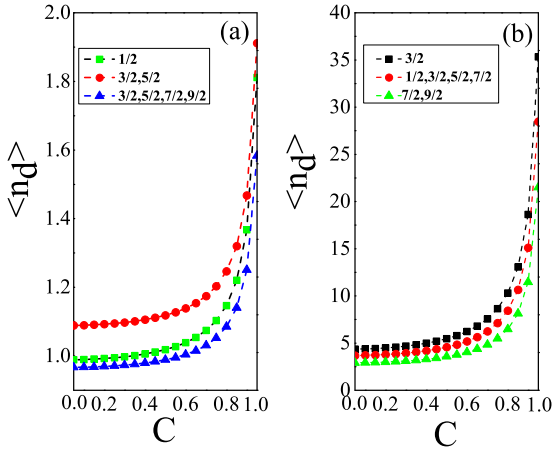

FIG. 6. (Color online) The expectation values of the d-boson number operator for the lowest states as a function of control parameter C for (a) a $j = 1/2$ particle coupled to a system of (s,d) bosons undergoing a U(5)-O(6) transition and (b) a single fermion with j = 3/2 coupled to a system of (s,d) bosons.

C. Expectation values of the d-boson number operator

An appropriate quantal order parameter is

$$\langle \hat{n_d} \rangle = \frac{\langle \psi | \hat{n_d} | \psi \rangle}{N}.$$

In order to obtain $\langle \hat{n_d} \rangle$, we let s_m^0 act on the eigenstate, $|k; \nu_s \nu n_\Delta L M\rangle$:

$$\langle \hat{n_d} \rangle = \frac{2\Lambda_1^0 - 2C^2\Lambda_0^0 + 2k\left(y_1^{-1} - C\right)}{1 - C^2} - \frac{5}{2N}. \qquad (27)$$

Figure 6(a) shows the expectation values of the d-boson number operator for states in which a $j = 1/2$ particle coupled to a system of (s,d) bosons undergoes a U(5)-O(6) transition as a function of control parameter C for $N = 10$ bosons. The expectation values of the d-boson number operator for states in which a $j = 3/2$ particle is coupled to a system of (s,d) bosons in terms of control parameter C are also shown in Fig. 6(b). Figure 6 displays that the expectation values of the number of d bosons for each J, n_d, remain approximately constant for $C < 0.45$ and only begin to change rapidly for $C > 0.45$. The near constancy of n_d for $C < 0.45$ is an obvious indication that U(5) dynamical symmetry is preserved in this region to a high degree and also the n_d values change rapidly with C over the range $0.65 \leqslant C \leqslant 1$. It can be seen from Fig. 6 that, due to the presence of the fermion, the transition is made sharper for $j = 1/2$ [Fig. 6(a)] while it is made smoother for $j = 3/2$ [Fig. 6(b)].

D. Energy differences

Figures 7(a) and 7(b) display continuous energy differences in terms of the control parameter, C, for states with a $j = 1/2$ particle coupled to a system of (s,d) bosons; that for $j = 3/2$ is shown in Figs. 7(c) and 7(d). Figure 7 shows that during the transition from one limit to another exist the points where energy is a minimum or a maximum near the critical point.

IV. EXPERIMENTAL EVIDENCE

This section presented the calculated results of low-lying states of the odd-A Ba and Rh isotopes. The results include energy levels and the $B(E2)$ values and two-neutron separation energies.

A. Energy spectrum

Nuclei in the mass regions around A $\sim$ 100 [27,28] and 130 [29] have transitional characteristics intermediate between spherical and γ-unstable shapes. The theoretical and experimental studies of energy spectra done in Refs. [28,30,31] show Rh and Ba isotopes have U(5) $\leftrightarrow$ O(6) transitional characteristics. The possible occurrence of this symmetry in $^{135}_{56}$Ba was recently suggested [30]. The negative-parity states in the odd-even nuclei Rh are built mainly on the $2p_{\frac{1}{2}}$ shell model orbit [28]. The single-particle orbits $1g_{\frac{7}{2}}$, $2d_{\frac{5}{2}}$, $2d_{\frac{3}{2}}$, and $3s_{\frac{1}{2}}$ establish the positive-parity states in odd-mass Ba isotopes [31]. In this study, a simplifying assumption is made that single-particle states are built on $j = 1/2$ and $j = 3/2$. We therefore analyze the negative-parity states of the odd-proton

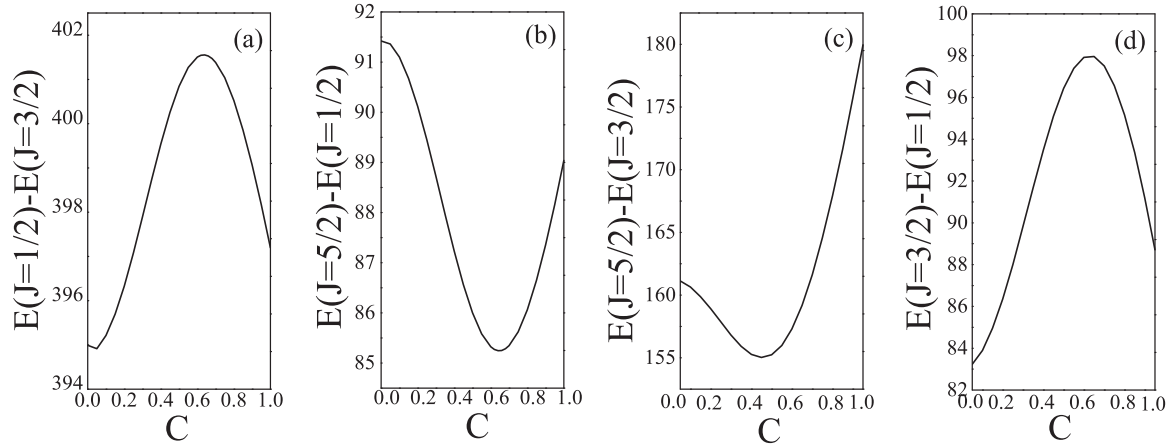

FIG. 7. Continuous energy differences (in keV) in terms of control parameter, C, for states having (a, b) $j = 3/2$ and (c, d) $j = 1/2$ particles coupled to a system of (s,d) bosons.

TABLE I. Parameters of Hamiltonian (11) used in the calculation of the Rh isotopes. All parameters are given in keV.

Nucleus	N	C	α	β	δ	γ	σ
$^{101}_{45}$Rh	5	0.06	105.99	4.2572	1.6782	1.2336	194.78
$^{103}_{45}$Rh	6	0.46	52	−1.053	1.5518	23.217	136.5
$^{105}_{45}$Rh	7	0.54	70.61	1.6273	8.7337	−0.0331	97.38
$^{107}_{45}$Rh	8	0.65	196.30	3.5077	−11.734	7.7931	120.48
$^{109}_{45}$Rh	9	0.7	245.269	2.438	−24.072	−181.02	184.79

nuclei, $^{101-109}_{45}$Rh, and positive-parity states of the odd-neutron nuclei, $^{127-137}_{56}$Ba. In order to obtain energy spectra and realistic calculations for these nuclei, we need to specify Hamiltonian parameters (11) and (12). Eigenvalues of these systems are obtained by solving Bethe ansatz equations with least-squares fitting processes to experimental data to obtain constants of the Hamiltonian. The best fits for the Hamiltonian's parameters, namely α, β, δ, and γ, used in the present work are shown in Tables I and II. Tables III(a)–III(e) and IV(a)–IV(f) show calculated energy spectra along with the experimental values. Figures 8 and 9 also show a comparison between the available experimental levels and the predictions of our results for the $^{101-109}_{45}$Rh and $^{127-137}_{56}$Ba isotopes in the low-lying region of spectra. An acceptable degree of agreement is obvious between them. We have tried to extract the best set of parameters that reproduce these complete spectra with minimum variations. It means that our suggestion to use this transitional Hamiltonian for the description of the Rh and Ba isotopic chain would not have any contradiction with other theoretical studies done with special hypotheses about mixing of intruder and normal configurations. However, predictions of our model for the control parameter of considered nuclei, C, describe the vibrational structure, i.e., $C = 0$, or rotational structure, namely $C = 1$, confirming the mixing of both vibrating and rotating structures in these nuclei when $C \sim 0.5 \rightarrow 0.65$. Figures 10 and 11 display a comparison between the calculated continuous energy differences and experimental data for Ba and Rh isotopes, respectively. It can be seen from the figures that our results for Ba isotopes are better than for Rh isotopes.

One of the most basic structural predictions of the $U^{BF}(5)$-$O^{BF}(6)$ transition is a $\frac{E(\nu_d=2)}{E(\nu_d=1)}$ value. The ratio equal to 2.2–2.3 indicates the spectrum of transitional nuclei [3,4,16,32]. Thus, we calculated this quantity for Rh and Ba isotopes. Figures 12(a) and 12(b) show $\frac{E(\nu_d=2)}{E(\nu_d=1)}$ prediction

TABLE II. Parameters of Hamiltonians (11) and (12) used in the calculation of the Ba isotopes. All parameters are given in keV.

Nucleus	N	C	α	β	δ	γ	σ
$^{127}_{56}$Ba	8	0.78	3.46	−0.0303	−1.1481	19.098	62.48
$^{129}_{56}$Ba	7	0.8	13.77	−2.685	−8.5776	15.69	94.25
$^{131}_{56}$Ba	6	0.77	0.578	−3.3839	−3.3319	27.12	128
$^{133}_{56}$Ba	5	0.68	21.37	−0.0274	16.46	−1.75	119
$^{135}_{56}$Ba	4	0.65	48.69	3.32		36.57	86.84
$^{137}_{56}$Ba	3	0.75	366	0.194		23.047	128.6

TABLE III(a). Energy spectra for $^{101}_{45}$Rh isotope.

$^{101}_{45}$Rh	J^π	K	ν_d	$E_{\rm exp}$ (keV)	$E_{\rm cal}$ (keV)
	$(1/2)^-_1$	2	0	0	0
	$(3/2)^-_1$	2	1	305.5	267.3
	$(5/2)^-_1$	2	1	305.5	273.5
	$(3/2)^-_2$	1	2	355.3	665.8
	$(5/2)^-_2$	1	2	355.3	671.9
	$(7/2)^-_1$	1	2	851.4	704.1
	$(9/2)^-_1$	1	2	851.4	715.2
	$(9/2)^-_2$	1	2	899.3	821.2
	$(5/2)^-_3$	2	1	996.4	794.6
	$(3/2)^-_4$	1	2	1058	997.9
	$(5/2)^-_4$	1	2	1058	971.8
	$(1/2)^-_2$	2	0	1531	1472.9

values for Ba and Rh isotopes, respectively. For Rh isotopes this value evolves from 2.1 to 2.8 while Ba isotopes vary from 2.85 to 1.9. Figure 12 displays that $\frac{E(\nu_d=2)}{E(\nu_d=1)}$ values for $^{105}_{45}$Rh and $^{133-135}_{56}$Ba isotopes are approximately 2.2–2.4.

B. $B(E2)$ transition

The observables such as electric quadrupole transition probabilities, $B(E2)$, as well as quadrupole moment ratios within the low-lying state provide important information about QPTs. In this section we discuss the calculation of $E2$ transition strengths and compare the results with the available experimental data. The electric quadrupole transition operator $\hat{T}^{(E2)}$ in odd-A nuclei consists of a bosonic and a fermionic part [8,27]:

$$\hat{T}^{(E2)} = \hat{T}^{(E2)}_B + \hat{T}^{(E2)}_F, \tag{28}$$

with

$$T^{(E2)}_{B,\mu} = q_2[s^+ \times \tilde{d} + d^+ \times \tilde{s}]^{(2)}_\mu + q'_2[d^+ \times \tilde{d}]^{(2)}_\mu = q_B Q_{B,\mu}, \tag{29}$$

$$Q_{B,\mu} = [s^+ \times \tilde{d} + d^+ \times \tilde{s}]^{(2)}_\mu + \chi[d^+ \times \tilde{d}]^{(2)}_\mu, \tag{30}$$

$$T^{(E2)}_F = q_f \sum_{jj'} Q_{jj'}[a^+_j \times \tilde{a}_{j'}]^{(2)}, \tag{31}$$

TABLE III(b). Energy spectra for the $^{103}_{45}$Rh isotope.

$^{103}_{45}$Rh	J^π	K	ν_d	$E_{\rm expt}$ (keV)	$E_{\rm calc}$ (keV)
	$(1/2)^-_1$	3	0	0	0
	$(3/2)^-_1$	2	1	294.984	334
	$(5/2)^-_1$	2	2	357.408	450.6
	$(1/2)^-_2$	3	0	803.07	598.6
	$(3/2)^-_2$	2	2	803.07	692.4
	$(7/2)^-_1$	2	2	847.58	705.4
	$(5/2)^-_2$	2	2	880.47	809
	$(9/2)^-_1$	2	2	920.1	915.3
	$(3/2)^-_3$	2	1	1277.04	1226.7
	$(13/2)^-_1$	1	3	1637.64	1576.5
	$(15/2)^-_1$	1	4	2221.2	2036.3
	$(17/2)^-_1$	1	4	2345.35	2432.6
	$(17/2)^-_2$	0	5	2418.6	2065.5

TABLE III(c). Energy spectra for the $^{105}_{45}$Rh isotope.

$^{105}_{45}$Rh	J^π	K	ν_d	$E_{\rm expt}$ (keV)	$E_{\rm calc}$ (keV)
	$(1/2)^-_1$	3	0	129.781	129.8
	$(3/2)^-_1$	3	1	392.65	229.2
	$(5/2)^-_1$	3	1	455.61	511.7
	$(3/2)^-_2$	2	2	762.11	811.2
	$(3/2)^-_3$	3	1	783	703.6
	$(5/2)^-_2$	2	2	817	821.7
	$(7/2)^-_1$	2	2	817	833.1
	$(5/2)^-_3$	2	3	866	868.2
	$(7/2)^-_2$	2	3	898	861.5
	$(7/2)^-_3$	2	3	976	937.9
	$(9/2)^-_1$	2	2	976	1043.5
	$(3/2)^-_4$	2	2	1147	1312.7
	$(5/2)^-_4$	2	2	1147	1311.9

where Q_B and $Q_{jj'}$ are the boson and fermion quadrupole operators and q_B and q_f are the effective boson and fermion charges [8,27]. In the $j = 1/2$ case, the $E2$ transitions are completely determined by the bosonic part of the $E2$ operator. The bosonic part has specific selection rules, where for the former term, $\Delta\nu_d = \pm 1$, $|\Delta L| \leqslant 2$ and for the latter, $\Delta\nu_d = 0, \pm 2$, $|\Delta L| \leqslant 0{,}4$. The reduced electric quadrupole transition rate between the $J_i \rightarrow J_f$ states is given by [8]

$$B(E2; \alpha_i J_i \rightarrow \alpha_f J_f) = \frac{|\langle \alpha_f J_f || T^{(E2)} || \alpha_i J_i \rangle|^2}{2J_i + 1}. \quad (32)$$

The electric quadrupole moment for a state with spin J is given by [8]

$$Q_J = \sqrt{\frac{16\pi}{5}} \left(\frac{J(2J-1)}{(2J+1)(J+1)(2J+3)} \right)^{\frac{1}{2}} \langle J || T^{(E2)} || J \rangle. \quad (33)$$

For evaluating $B(E2)$, we consider eigenstates Eq. (14) where the normalization factor is obtained as

$$\mathcal{N} = \sqrt{\frac{1}{\prod_{p=1}^{k} \sum_{i=p}^{k} \left(\frac{2C^2(k-p+\frac{1}{2}(\nu_s+\frac{1}{2}))}{(1-C^2 y_{k+1-p})(1-C^2 y_i)} + \frac{2(k-p+\frac{1}{2}(\nu_d+\frac{5}{2}))}{(1-y_{k+1-p})(1-y_i)} \right)}}. \quad (34)$$

TABLE III(d). Energy spectra for the $^{107}_{45}$Rh isotope.

$^{107}_{45}$Rh	J^π	K	ν_d	$E_{\rm expt}$ (keV)	$E_{\rm calc}$ (keV)
	$(1/2)^-_1$	4	0	268.36	268.4
	$(3/2)^-_1$	3	1	485.66	345.4
	$(5/2)^-_1$	3	1	543.84	410.9
	$(9/2)^-_1$	3	2	559.97	423.4
	$(3/2)^-_2$	3	2	752.55	818.8
	$(5/2)^-_2$	3	2	877.75	870.4
	$(3/2)^-_3$	3	1	974.44	921.9
	$(5/2)^-_3$	2	3	974.44	958.6
	$(7/2)^-_1$	3	2	974.44	780.9
	$(3/2)^-_4$	3	2	1009.76	1016.3
	$(5/2)^-_4$	3	2	1009.76	1055.3
	$(7/2)^-_2$	2	3	1251	1099.5
	$(1/2)^-_2$	4	0	1334	1431.2

TABLE III(e). Energy spectra for the $^{109}_{45}$Rh isotope.

$^{109}_{45}$Rh	J^π	K	ν_d	$E_{\rm expt}$ (keV)	$E_{\rm calc}$ (keV)
	$(1/2)^-_1$	4	0	374.1	374.1
	$(3/2)^-_1$	4	1	568.2	436.6
	$(5/2)^-_1$	4	1	623.2	401.5
	$(3/2)^-_2$	3	2	704.9	758.1
	$(5/2)^-_2$	3	2	856.1	819.6
	$(5/2)^-_3$	3	3	926.9	827.6
	$(3/2)^-_3$	4	1	1162.3	1378.8
	$(3/2)^-_4$	3	2	1214.3	1003.3
	$(5/2)^-_4$	3	2	1283.9	985.6
	$(1/2)^-_2$	4	0	1631	1876.6
	$(3/2)^-_5$	4	1	1631	1627.4
	$(1/2)^-_3$	4	0	1753	1703
	$(3/2)^-_6$	4	1	1753	1750

Unfortunately there are very few experimental data available on electromagnetic properties for odd-mass Ba [31] and Rh [27] isotopes. The values of effective charge (q_B,q_f) are listed in Table V. Table VI shows experimental and calculated values for $B(E2)$ for negative-parity states of $^{103}_{45}$Rh and positive-parity states of $^{135}_{56}$Ba. The quadrupole moments for $^{103}_{45}$Rh and $^{135}_{56}$Ba are also displayed in Table VII. Tables VI and VII show that in general there is good agreement between the calculated $B(E2)$ values and the quadrupole moments with the experimental data.

The values of the control parameter, C, suggest structural changes in nuclear deformation and shape-phase transitions in odd-proton Rh isotopes and odd-neutron Ba isotopes. Because of the effect of a single nucleon on the transition and especially the critical point, exact selection of the critical point is difficult.

TABLE IV(a). Energy spectra for the $^{127}_{56}$Ba isotope.

$^{127}_{56}$Ba	J^π	K	ν_d	$E_{\rm expt}$ (keV)	$E_{\rm calc}$ (keV)
	$(1/2)^+_1$	4	0	0	0
	$(3/2)^+_1$	3	1	56.1	51.4
	$(5/2)^+_1$	3	1	81	146.9
	$(7/2)^+_1$	3	2	195.1	265.7
	$(3/2)^+_2$	3	2	269.5	256.3
	$(5/2)^+_2$	3	2	269.5	237.2
	$(7/2)^+_1$	2	3	324.1	376.3
	$(7/2)^+_2$	2	3	374.9	367.1
	$(9/2)^+_1$	3	2	415.6	526.1
	$(11/2)^+_1$	2	3	668.9	723.8
	$(11/2)^+_2$	2	4	867.9	759.4
	$(13/2)^+_1$	2	3	963.6	972.1
	$(15/2)^+_1$	2	4	1291.2	1259.8
	$(15/2)^+_2$	1	5	1519.6	1425.5
		2	4	1654.4	1584.4

TABLE IV(b). Energy spectra for the $^{129}_{56}$Ba isotope.

$^{129}_{56}$Ba	J^π	K	ν_d	E_{expt} (keV)	E_{calc} (keV)
	$(1/2)^+_1$	3	0	0	0
	$(7/2)^+_1$	2	2	8.42	48.71
	$(3/2)^+_1$	3	1	110.56	185.67
	$(3/2)^+_2$	2	2	253.77	210.76
	$(9/2)^+_1$	2	2	263.1	249.9
	$(1/2)^+_2$	3	0	278.58	331.88
	$(3/2)^+_3$	3	1	278.58	228.15
	$(5/2)^+_1$	3	1	278.58	292.83
	$(5/2)^+_2$	2	2	318.4	290.66
	$(3/2)^+_4$	2	2	457.03	483.53
	$(3/2)^+_5$	3	1	459.29	492.44
	$(5/2)^+_3$	2	3	459.29	548.4
	$(7/2)^+_2$	2	3	467.3	589.6
	$(11/2)^+_1$	2	3	544.7	441.257
	$(13/2)^+_1$	2	3	864.1	918.66

TABLE IV(c). Energy spectra for the $^{131}_{56}$Ba isotope.

$^{131}_{56}$Ba	J^π	K	ν_d	E_{expt} (keV)	E_{calc} (keV)
	$(1/2)^+_1$	3	0	0	0
	$(3/2)^+_1$	2	1	108.08	70.5
	$(3/2)^+_2$	2	2	285.25	359.2
	$(5/2)^+_1$	2	1	316.587	424.7
	$(1/2)^+_2$	3	0	365.16	487.8
	$(3/2)^+_3$	2	1	525.85	577.3
	$(5/2)^+_2$	2	2	525.85	494.8
	$(7/2)^+_1$	2	2	543.11	638.1
	$(3/2)^+_4$	2	1	561.752	643.5
	$(5/2)^+_3$	1	3	561.75	473.3
	$(3/2)^+_5$	0	5	718.78	573.7
	$(5/2)^+_4$	2	1	718.78	778.6
	$(1/2)^+_2$	1	3	719.49	698.1
	$(15/2)^+_1$	1	4	1796.4	1821.6
	$(17/2)^+_1$	1	4	2121.7	2282.6

TABLE IV(d). Energy spectra for the $^{133}_{56}$Ba isotope.

$^{133}_{56}$Ba	J^π	K	ν_d	E_{expt} (keV)	E_{calc} (keV)
	$(1/2)^+_1$	2	0	0	0
	$(3/2)^+_1$	2	1	12.3	64.86
	$(5/2)^+_1$	2	1	291.2	175.93
	$(3/2)^+_2$	1	2	302.4	419.34
	$(1/2)^+_2$	1	2	539.8	443.23
	$(7/2)^+_1$	1	2	577.5	701.22
	$(3/2)^+_3$	1	3	630.6	705.24
	$(5/2)^+_2$	1	2	630.6	720.84
	$(5/2)^+_3$	1	3	676.5	675.45
	$(3/2)^+_4$	0	5	676.5	726.015
	$(5/2)^+_4$	1	3	858.5	696.45
	$(9/2)^+_1$	1	2	883.3	933.86
	$(7/2)^+_2$	1	3	1112.3	938.98

TABLE IV(e). Energy spectra for the $^{135}_{56}$Ba isotope.

$^{135}_{56}$Ba	J^π	K	ν_d	E_{expt} (keV)	E_{calc} (keV)
	$(3/2)^+_1$	2	0	0	0
	$(1/2)^+_1$	1	1	220.954	200.66
	$(5/2)^+_1$	1	1	480.52	502.31
	$(3/2)^+_2$	1	1	587.82	696.93
	$(3/2)^+_3$	2	0	855	866.9
	$(1/2)^+_2$	1	2	910.35	985.569
	$(5/2)^+_2$	1	2	979.966	904.815
	$(3/2)^+_4$	1	2	979.969	1145.37

In considering this problem, we proposed $C \sim 0.5$–0.65 as the critical point. So, we conclude from the values of the control parameter that were obtained, the $\frac{E(\nu_d=2)}{E(\nu_d=1)}$ value, and energy differences that $^{105}_{45}$Rh and $^{133-135}_{56}$Ba isotopes are the best candidates for $U^{BF}(5)$-$O^{BF}(6)$ transition. Phase transitions from the spherical to the γ-unstable limit for odd nuclei in the frameworks of the IBFM and the Bohr collective model, with the odd nucleon lying in a $j = 3/2$ shell, were considered in Refs. [11,15,16]. So, it must be useful and worthwhile to compare the present method and results to the method and results of these papers. The paper by Alonso *et al.* [11] investigated the phase transition around the critical point in the evolution from spherical to γ-unstable shapes in the case where an odd $j = 3/2$ particle coupled to an even-even boson core that undergoes a transition from the spherical U(5) to the γ-unstable O(6) situation. They used the coherent state formalism and semiclassical approach to get energy eigenvalues, whereas our method for obtaining spectra is quantal. We also investigated the transition from the spherical to the γ-unstable limit in odd-A nuclei when only the boson core experiences the transition and fermions with $j = 1/2$ and $3/2$ are coupled to boson core. In our work, the eigenstates and energy eigenvalues for the transitional region were evaluated by using the dual algebraic structure, the Richardson-Gaudin method, and affine $\widehat{SU(1,1)}$ Lie algebra; thus, the natures of the two schemes are completely different. They obtained energy

TABLE IV(f). Energy spectra for the $^{137}_{56}$Ba isotope.

$^{137}_{56}$Ba	J^π	K	ν_d	E_{expt} (keV)	E_{calc} (keV)
	$(3/2)^+_1$	2	0	0	0
	$(7/2)^+_1$	1	1	1252.5	1093.9
	$(5/2)^+_1$	1	1	1294	1124.25
	$(3/2)^+_2$	1	1	1463.8	1607
	$(1/2)^+_1$	1	2	1857	1782.9
	$(1/2)^+_2$	1	1	1836.2	1899.2
	$(3/2)^+_3$	2	0	2041	1940.4
	$(5/2)^+_2$	1	2	1899	2063.2
	$(3/2)^+_4$	1	2	1899	1883.5
	$(5/2)^+_3$	1	2	2041	2041.8
	$(7/2)^+_2$	1	2	2230	2258
	$(9/2)^+_1$	1	2	2230	2248.6
	$(7/2)^+_3$	1	2	2340	2263.5
	$(7/2)^+_4$	1	1	2423.8	2530

TABLE V. The coefficients of $T(E_2)$ used in the present work for $^{103}_{45}$Rh and $^{135}_{56}$Ba isotopes.

Nucleus	q_B (eb)	q_f (eb)
$^{103}_{45}$Rh	0.461	0
$^{135}_{56}$Ba	4.7329	−0.7194

spectra and electromagnetic transitions in the critical point and their displayed results are also in qualitative agreement with the proposed E(5/4) model [15]. They showed that energy spectra and electromagnetic transitions, in correspondence with the critical point, display behaviors qualitatively similar to those of the even core. We investigated the change in level structure induced by the phase transition (Figs. 3–7) by doing a quantal analysis (Sec. III). In order to exhibit the qualitative features of our model, we presented extensive numerical results. New experimental data on Ba and Rh isotopes were used to test the predictions of the scheme in dynamical symmetry limits and the transition region. We presented experimental evidence for the Bose-Fermi critical symmetry in Ba and Rh isotopes. Iachello [15] extended the concept of critical symmetry to critical supersymmetry and provided a benchmark for the study of odd-even nuclei in most situations in which the system is undergoing a phase transition between two different phases (shapes). A special solution, called E(5/4), for odd-even nuclei in the transitional region between spherical and γ-unstable shapes was introduced. The energy spectrum and electromagnetic transitions were obtained for the odd-A nuclei in critical point symmetry. In this paper, the states in $^{133}_{56}$Ba built on the single-particle neutron level $d_{3/2}$ were considered an E(5/4) candidate. We also investigated $^{133}_{56}$Ba in a state where the odd nucleon is in a $j = 1/2$ shell and showed that $^{133}_{56}$Ba can be considered as the Bose-Fermi critical symmetry. Caprio and Iachello [16] obtained analytic descriptions for transitional nuclei near the critical point. The solutions provided baselines for experimental studies of even-even [E(5)] and odd-mass [E(5/4)] nuclei near the critical point of the spherical to γ-unstable phase transition. They concentrated upon those distinguishing observables that vary along the U(5)-O(6) transition. The observables such as the energy ratios and the $B(E2)$ strength ratios are the most sensitive to the U(5)-O(6) structural transition. Their results provided benchmarks for nuclei near the critical point of the U(5)-O(6) phase transition and can be used as a basis for comparison with experiment. So, we also presented experimental evidence for the U(5)-O(6) transition for negative-parity states of the $^{101-109}_{45}$Rh isotopic chain and positive-parity states of the $^{127-137}_{56}$Ba isotopic chain and performed an analysis for these isotopes. We calculated the energy ratio quantity for Rh and Ba isotopes by using Caprio's study [16].

C. Two-neutron separation energies

Shape-phase transitions in nuclei can be studied experimentally by considering the behavior of the ground-state energies of a series of isotopes, or, more conveniently, the behavior of the two-neutron separation energies, S_{2n} [2].

TABLE VI. $B(E2)$ values for $^{103}_{45}$Rh and $^{135}_{56}$Ba isotopes. The experimental data for the $^{103}_{45}$Rh isotope are taken from Refs. [23,27]. The experimental data for the $^{135}_{56}$Ba isotope are taken from Refs. [23,33].

Nucleus	$J_i^\pi \rightarrow J_j^\pi$	$B(E_2(e^2b^2)$	
		Expt.	Calc.
$^{103}_{45}$Rh	$(3/2)^-_1 \rightarrow (1/2)^-_1$	0.109	0.1172
	$(5/2)^-_1 \rightarrow (1/2)^-_1$	0.118	0.1172
	$(5/2)^-_2 \rightarrow (1/2)^-_1$	0.0044	0.0044
	$(5/2)^-_2 \rightarrow (3/2)^-_1$	0.0768	0.0645
	$(5/2)^-_2 \rightarrow (5/2)^-_1$	0.015	0.0097
	$(7/2)^-_1 \rightarrow (3/2)^-_1$	0.13	0.1165
	$(9/2)^-_1 \rightarrow (5/2)^-_1$	0.179	0.1349
$^{135}_{56}$Ba	$(1/2)^+_1 \rightarrow (3/2)^+_1$	4.6	3.696
	$(5/2)^+_1 \rightarrow (1/2)^+_1$	2.65	2.913
	$(7/2)^+_1 \rightarrow (3/2)^+_1$	19.9	14.784
	$(1/2)^+_2 \rightarrow (3/2)^+_1$	11.7	14.403
	$(3/2)^+_2 \rightarrow (3/2)^+_1$	18	14.785
	$(3/2)^+_3 \rightarrow (3/2)^+_1$	7	7.001

However, the ground-state two-neutron separation energies, S_{2n}, are observables that are very sensitive to the details of the nuclear structure. The occurrence of continuities in the behavior of two-neutron separation energies describe a second-order shape-phase transition between spherical and γ-unstable rotor limits [2,34]. We investigated the evolution of two-neutron separation energies along the Ba and Rh isotopic chains by both experimental and theoretical values, which are presented in Fig. 13. The binding energy as a function of proton and neutron number is given by [2]

$$E_B(N_\pi, N_\nu) = E_c + A_\pi N_\pi + A_\nu N_\nu + \tfrac{1}{2}B_\pi N_\pi(N_\pi - 1) + \tfrac{1}{2}B_\nu N_\nu(N_\nu - 1) + C N_\pi N_\nu + E_D(N_\pi, N_\nu), \quad (35)$$

where N_π (N_ν) is the number of proton (neutron) bosons in the valence shell, E_c is the contribution from the core, and E_D is the contribution to the binding energy due to the deformation.

TABLE VII. Quadrupole moments for $^{103}_{45}$Rh and $^{135}_{56}$Ba isotopes. The experimental data for the $^{103}_{45}$Rh isotope are taken from Refs. [23,27]. The experimental data for the $^{135}_{56}$Ba isotope are taken from Refs. [23,33].

Nucleus	J^π	Q (eb)	
		Expt.	Calc.
$^{103}_{45}$Rh	$(1/2)^-_1$	0	0
	$(3/2)^-_1$	−0.32	−0.2588
	$(5/2)^-_1$	−0. 41	−0.2824
	$(7/2)^-_1$		−0.5538
	$(9/2)^-_1$		−0.5355
$^{135}_{56}$Ba	$(3/2)^+_1$	0.146	0.1509
	$(1/2)^+_1$		0.1349
	$(5/2)^+_1$		0.5126

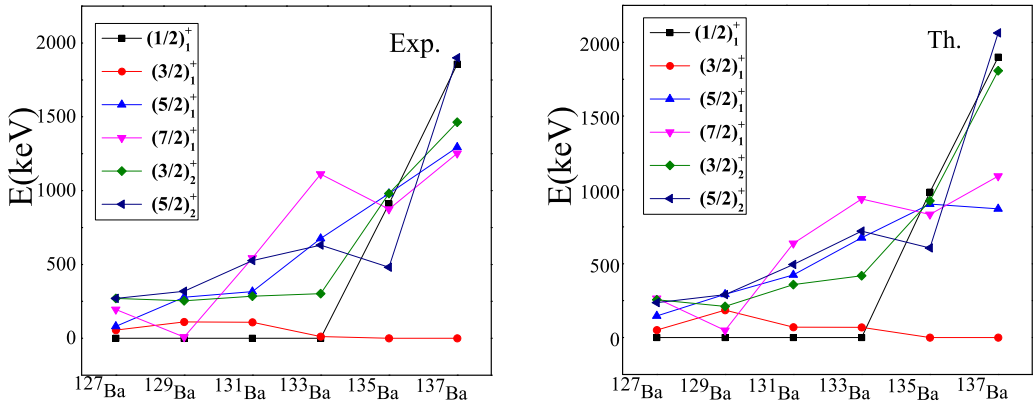

FIG. 8. (Color online) Experimental and calculated energies (in keV) for the low-lying positive-parity states of odd-A Ba isotopes. The parameters of the calculation are given in Table II. The experimental data are taken from Ref. [23].

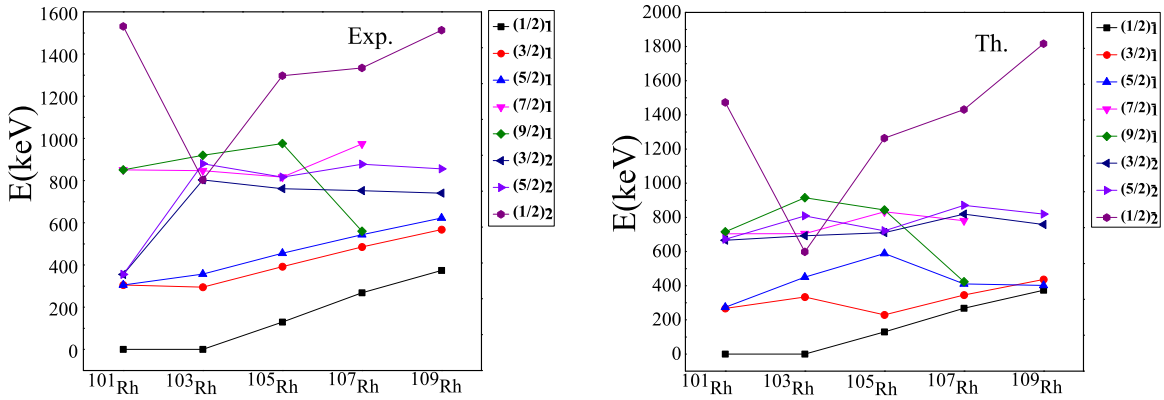

FIG. 9. (Color online) Experimental and calculated energies (in keV) for the low-lying negative-parity states of odd-even Rh isotopes. The parameters of the calculation are given in Table I. The experimental data are taken from Ref. [23].

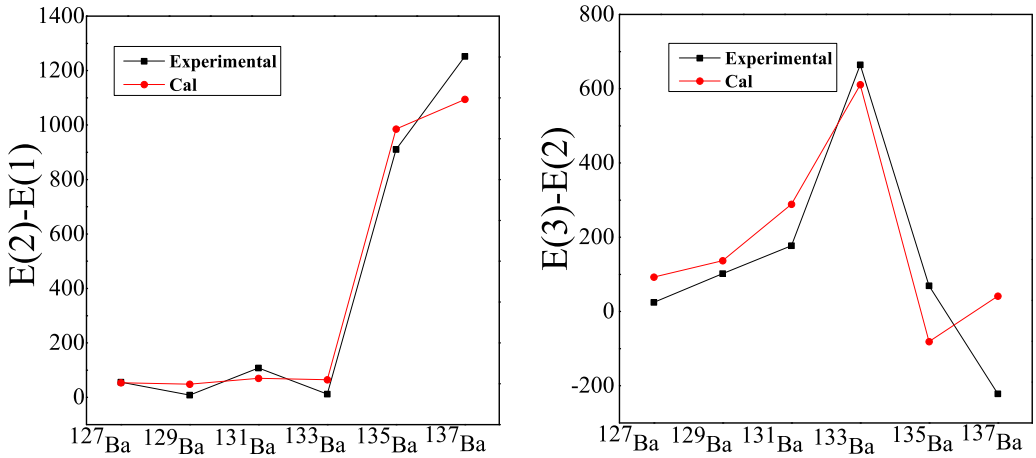

FIG. 10. (Color online) A comparison between the calculated continuous energy differences and experimental data for Ba. The experimental data are taken from Ref. [23].

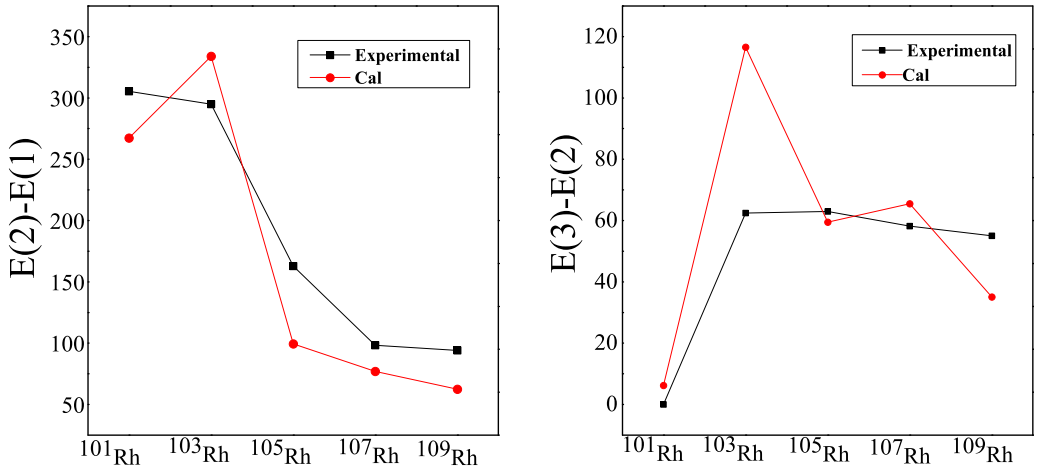

FIG. 11. (Color online) A comparison between the calculated continuous energy differences and experimental data for Rh. The experimental data are taken from Ref. [23].

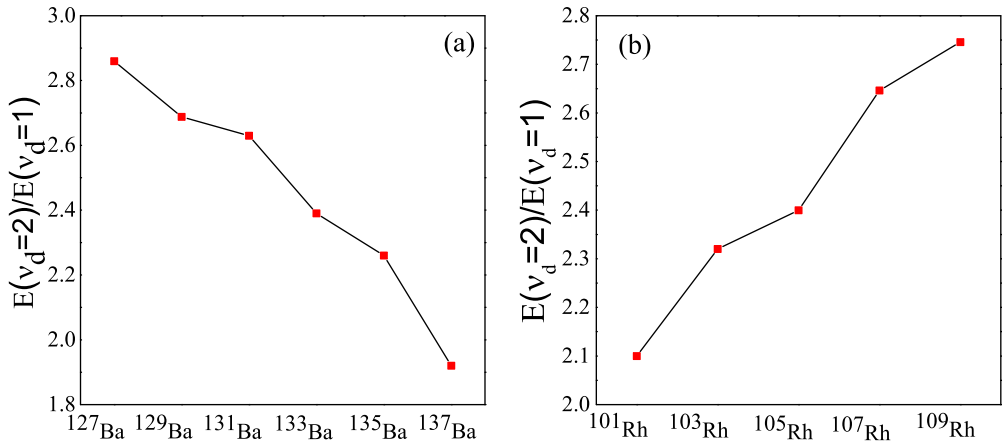

FIG. 12. (Color online) $(E(v_d = 2))/(E(v_d = 1))$ prediction values for (a) odd-A Ba isotopes and (b) odd-even Rh isotopes. The experimental data are taken from Ref. [23].

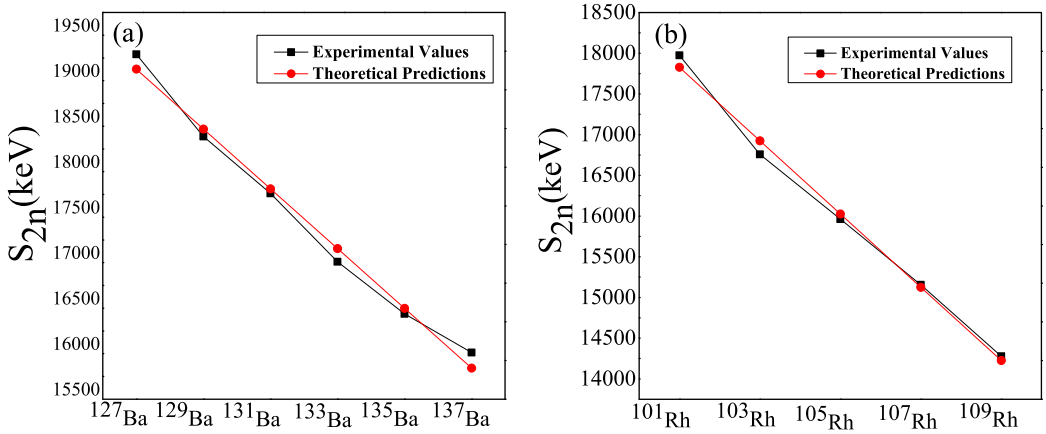

FIG. 13. (Color online) A comparison between theoretical and experimental two-neutron separation energies, S_{2n} (in keV) for (a) Ba isotopes and (b) Rh isotopes. The experimental data are taken from Ref. [23].

Using Eq. (35), one obtains the following relation for the two-neutron separation energy [2]:

$$\begin{aligned} S_{2n}(N_\pi, N_\nu) &= E_B(N_\pi, N_\nu) - E_B(N_\pi, N_\nu - 1) \\ &= A_n + BN_\pi + C_n N_\nu + [E_D(N_\pi, N_\nu) \\ &\quad - E_D(N_\pi, N_\nu - 1)]. \end{aligned} \tag{36}$$

Using the S_{2n} empirical values for these isotopic chains [23], we extracted $A_n + BN_\pi = 15.1857, 20.526$ MeV and $C_n = 1.9784, -1.7992$ MeV for Ba and Rh, respectively. Then, we obtained the two-neutron separation energies, which are shown in Fig. 13, together with the experimental values. It can be seen from Fig. 13 that there exist continuities (linear variation) in the behavior of two-neutron separation energies; thus, the phase transition for Ba and Rh isotopic chains is of second order. Our result confirmed the predictions made in Refs. [2,34], where they suggest a linear variation of S_{2n} with respect to the neutron number for the U(5)-SO(6) transitional region.

V. CONCLUSIONS

We analyzed the transition from spherical to γ-unstable shapes in odd-A nuclei. Key observables of the phase transition such as level crossing, ground-state energy and derivative of the ground-state energy, and expectation values of the d-boson number operator were calculated. We presented experimental evidence for the U(5)-O(6) transition for negative-parity states of the $^{101-109}_{45}$Rh isotopic chain and positive-parity states of $^{127-137}_{56}$Ba isotopic chain, and performed an analysis for these isotopes via a SU(1,1)-based Hamiltonian. The results indicate that the energy spectra of the Rh and Ba isotopes can be reproduced quite well. The calculated $B(E2)$ values and two-neutron separation energies are in agreement with the available experimental data. Our results show that Rh isotopes have γ-unstable rotor features but the vibrational character is dominant, while a dominance of dynamical symmetry O(6) exists for the Ba isotopic chain and also $^{105}_{45}$Rh and $^{133-135}_{56}$Ba isotopes are the best candidates for the $U^{BF}(5)$-$O^{BF}(6)$ transition.

[1] D. Rowe, Nucl. Phys. A **745**, 47 (2004).
[2] F. Iachello and A. Arima, *The Interacting Boson Model* (Cambridge University Press, Cambridge, UK, 1987).
[3] F. Iachello, Phys. Rev. Lett. **85**, 3580 (2000).
[4] F. Iachello, Phys. Rev. Lett. **87**, 052502 (2001).
[5] D. H. Feng, R. Gilmore, and S. R. Deans, Phys. Rev. C **23**, 1254 (1981).
[6] P. Cejnar, J. Jolie, and R. F. Casten, Rev. Mod. Phys. **82**, 2155 (2010).
[7] F. Iachello, Phys. Rev. Lett. **91**, 132502 (2003).
[8] F. Iachello and P. Van Isacker, *The Interacting Boson-Fermion Model* (Cambridge University Press, Cambridge, UK, 1991).
[9] R. Bijker and A. E. L. Dieperink, Nucl. Phys. A **379**, 221 (1982).
[10] O. Scholten and N. Blasi, Nucl. Phys. A **380**, 509 (1982).
[11] C. E. Alonso, J. M. Arias, L. Fortunato, and A. Vitturi, Phys. Rev. C **72**, 061302(R) (2005).
[12] C. E. Alonso, J. M. Arias, and A. Vitturi, Phys. Rev. C **75**, 064316 (2007).
[13] C. E. Alonso, J. M. Arias, L. Fortunato, and A. Vitturi, Phys. Rev. C **79**, 014306 (2009).
[14] M. Boyukata, C. E. Alonso, J. M. Arias, L. Fortunato, and A. Vitturi, Phys. Rev. C **82**, 014317 (2010).
[15] F. Iachello, Phys. Rev. Lett. **95**, 052503 (2005).
[16] M. Caprio and F. Iachello, Nucl. Phys. A **781**, 26 (2007).
[17] F. Iachello, A. Leviatan, and D. Petrellis, Phys. Lett. B **705**, 379 (2011).
[18] M. A. Jafarizadeh, N. Fouladi, H. Sabri, and B. R. Maleki, Nucl. Phys. A **890–891**, 29 (2012).
[19] F. Pan and J. Draayer, Nucl. Phys. A **636**, 156 (1998).
[20] F. Pan, X. Zhang, and J. Draayer, J. Phys. A: Math. Gen. **35**, 7173 (2002).
[21] M. Caprio, J. Skrabacz, and F. Iachello, J. Phys. A: Math. Theor. **44**, 075303 (2011).
[22] D. Rowe, M. Carvalho, and J. Repka, Rev. Mod. Phys. **84**, 711 (2012).
[23] National Nuclear Data Center, http://www.nndc.bnl.gov/chart/reColor.jspnewColor=dm.
[24] J. Jolie, S. Heinze, P. Van Isacker, and R. F. Casten, Phys. Rev. C **70**, 011305(R) (2004).
[25] D. Petrellis, A. Leviatan, and F. Iachello, Ann. Phys. **326**, 926 (2011).
[26] E. Williams, R. J. Casperson, and V. Werner, Phys. Rev. C **81**, 054306 (2010).
[27] G. Maino, A. Ventura, A. Bizzeti-Sona, and P. Blasi, Z. Phys. A **340**, 241 (1991).
[28] J. Arias, C. Alonso, and M. Lozano, Nucl. Phys. A **466**, 295 (1987).
[29] S. Abu-Musleh, H. Abu-Zeid, and O. Scholten, Nucl. Phys. A **927**, 91 (2014).
[30] M. Fetea, R. Cakirli, R. Casten, D. Warner, E. McCutchan, D. Meyer, A. Heinz, H. Ai, G. Gurdal, J. Qian, and R. Winkler, Phys. Rev. C **73**, 051301 (2006).
[31] C. Alonso, J. Arias, and M. Lozano, J. Phys. G **13**, 1269 (1987).
[32] R. Casten and E. McCutchan, J. Phys. G: Nucl. Part. Phys. **34**, R285 (2007).
[33] B. Singh, A. A. Rodionov, and Y. L. Khazov, Nucl. Data Sheets **109**, 517 (2008).
[34] N. V. Zamfir, S. Anghel, and G. Cata-Danil, AIP Conf. Proc. No. 1072, 118 (AIP, New York, 2008).